Calcium Photorelease from a Symmetrical Donor−Acceptor−Donor Bis-crown-fluoroionophore Evidenced by Ultrafast Absorption Spectroscopy

Nathalie Marcotte,[†] Pascal Plaza,*[,‡] Dominique Lavabre,[†] Suzanne Fery-Forgues,*[,†] and Monique M. Martin[‡]

Laboratoire des Interactions Moléculaires Réactivité Chimique et Photochimique (CNRS UMR 5623), Université Paul Sabatier, 118 route de Narbonne, 31062 Toulouse Cedex, France, and Laboratoire P. A. S. T. E. U. R. (CNRS UMR 8640), Département de Chimie, Ecole Normale Supérieure, 24 rue Lhomond, 75231 Paris Cedex 05, France

Received: November 19, 2002

The excited-state properties of a calcium dicomplex (AM_2) of 2,5-[bis-[4*N*-(aza-15-crown-5)phenyl]methylene]-cyclopentanone (**A**) in acetonitrile are investigated by ultrafast absorption spectroscopy. Spectroscopic evidence of an ultrafast cation decoordination following subpicosecond excitation of the chromophore is given. A global analysis of the time-resolved data is performed, and a kinetic scheme is tentatively proposed, which quantitatively describes the dynamics of the deactivation pathway of the AM_2 dicomplex. A first step would involve the disruption of one of the two nitrogen−calcium bonds at a rate constant of 4×10^{11} s^{-1}, followed by the diffusion of the cation out of the crown at a rate of 5.8×10^{10} s^{-1}. The resulting AM complex would then relax both to its ground state (5.4×10^{8} s^{-1}) and to its triplet state (2.8×10^{8} s^{-1}).

Introduction

Supramolecular systems designed to recognize metal ions are of great interest in the fields of chemical, environmental, and biological analysis. These chemosensors typically combine two subunits: a receptor moiety that selectively binds the target substrate and a sensor moiety, usually a chromophore or a fluorophore, that signals the occurrence of the recognition.[1−7] Making use of fluorescence ensures a specially high sensitivity and permits the signal transduction to be characterized by both intensity ratios and lifetime measurements. In one of the approaches commonly employed for the design of fluorescent sensors, the receptor is an integral part of a conjugated π system; these are intrinsic fluoroionophores. Most of the intrinsic fluoroionophores studied to date are built on organic molecules of the electron donor−acceptor type, exhibiting an intramolecular charge transfer (ICT) transition upon irradiation by light. The interaction of the cation with the donor or the acceptor group alters the ICT efficiency so that changes can be observed on both absorption and fluorescence spectra.[1,8]

When the receptor is an azacrown group, the nitrogen atom plays the role of electron donor for both the ICT process and the cation complexation.[9,10] Complexation induces a blue shift of the absorption band due to a reduction of the length of the conjugated system.[8] The major effect of cation binding on the fluorescence spectrum is a change in intensity, the observed enhancement[11−13] or decrease[9,10] depending on the particular photophysical mechanism involved in the fluorophore relaxation. The position of the emission band often remains unchanged or is at most slightly blue-shifted. The latter behavior is quite surprising and has been attributed to a decoordination reaction in the excited state. Actually, some research groups showed that the deactivation mechanism of the excited complex involves a disruption of the nitrogen−cation bond,[14−19] which can further give rise to cation release to the bulk.[20] Such a photorelease would be essential for the spatial and temporal control of a wide variety of biological functions through fast local jumps of some intracellular cation (in particular Ca^{2+}) concentration.[21] Until now, most of the phototriggers used for the release of biologically active compounds are based on the photocleavage of a labile group.[22−26] However, the use of an intrinsic fluoroionophore could allow a reversible complexation leading to a major improvement of the S/N ratio by accumulation of the experiment over a large number of laser shots. The first studies on this topic have independently been performed by Martin et al. on a crowned merocyanine dye (DCM-crown)[14] and by Dumon et al. on some crown-stilbene derivatives.[17] For DCM-crown, a disruption of the nitrogen−cation bond in the locally excited state of the complex is followed by an intramolecular charge transfer concerted with the cation departure (early release) within a few picoseconds.[15,16] The decoordination pathway of DCS-crown (a crown-cyanostilbene) also implies a fast dissociation of the nitrogen−cation bond followed by the formation of a solvent-separated cation−probe pair in the picosecond time scale.[18,19] As far as the complete photorelease of cations to the bulk is concerned, a recent experiment on DCM-crown complexed with Sr^{2+} evidenced a subnanosecond process leading to a long-lived photoejected cation.[20]

Compared to standard electron donor−acceptor systems, molecules containing two electron-donating groups and a single acceptor group on the same conjugated π systems (D−A−D systems) have principally been investigated for their potential use in optoelectronics because of their nonlinear optical properties,[27−31] and less attention has been paid to their use as ion probes.[32,33] A dimethylaminobenzoxazinone derivative, the emission of which was enhanced and strongly shifted to the blue in the presence of cations, was first reported by Valeur's

* To whom correspondence should be addressed. Fax numbers: (+33) 1 44 32 33 25 (P. Plaza); (+33) 5 61 55 81 55 (S. Fery-Forgues). E-mail addresses: Pascal.Plaza@ens.fr (P. Plaza); sff@chimie.ups-tlse.fr (S. Fery-Forgues).

[†] Université Paul Sabatier.

[‡] Ecole Normale Supérieure.

10.1021/jp027495u CCC: $25.00
Published on Web 03/14/2003

SCHEME 1: Chemical Structure of Compound A

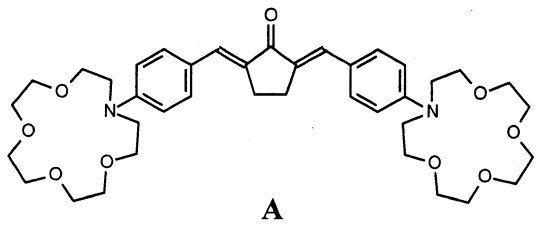

A

team.[32] Recently, Rurack et al studied the influence of the same second donor, a dimethylamino group, on the spectroscopic properties of a crown-benzothiazole derivative.[33] The emission spectrum of this $D-A-D_{(crown)}$ system was reported to be red-shifted and drastically enhanced upon cation complexation. This was rationalized by the conversion of the donor character of the azacrown into an acceptor character, yielding a $D-A-A_{(bound\ crown)}$ pattern. This pattern prevents the cation decoordination in the excited state and exhibits an intense CT emission. Few fluoroionophores bearing two *N*-aza-crown groups have been investigated and their potential activity as photoreleasers has not yet been addressed. One can mention a phenanthroline derivative,[34] some squaraine dyes,[35−37] and ketocyanine derivatives recently studied by some of us[38,39] and by others.[40,41] These ketocyanine dyes exhibit a red-shifted emission and a large decrease in the fluorescence quantum yield upon cation binding. Because the diphenylpentadienone derivative was shown to exist in solution as a mixture of rotational isomers,[42] we preferred to investigate here the rigid analogue, 2,5-[bis-[4*N*-(aza-15-crown-5)phenyl]methylene]cyclopentanone (**A**) (Scheme 1). We present here a photophysical study of **A** in acetonitrile, free and complexed by two calcium ions, by steady-state and subpicosecond transient absorption spectroscopy. Our aim is at better understanding the complexing and mainly the photodecomplexing behavior of this symmetrical system. Special attention is paid to modeling the mechanism involved in the decomplexation process of the AM_2 dicomplex, by a global fitting of the kinetic data.

Experimental Section

Materials. Spectrophotometric grade acetonitrile (Merck) was used for absorption and fluorescence measurements. Calcium perchlorate ($Ca(ClO_4)_2 \cdot 4H_2O$) from Aldrich was used as received.

Synthesis. 2,5-[Bis-[4*N*-(aza-15-crown-5)phenyl]methylene]-cyclopentanone (**A**) was prepared according to a general procedure previously described.[38] In brief, *N*-phenylaza-15-crown-5 was formylated according to the general procedure of Dix and Vögtle[43] and the crowned aldehyde was then condensed in basic medium with cyclopentanone by the method of Olomucki and Le Gall.[44] The oily product was purified by flash column chromatography on silica using 95% ethanol as eluent.

Apparatus. UV/vis absorption spectra were recorded on a Hewlett-Packard 8452 A diode array spectrophotometer. Steady-state fluorimetry was performed on a Photon Technology International (PTI) Quanta Master 1 spectrofluorometer. All fluorescence spectra presented here were corrected. The fluorescence quantum yields were determined using coumarin 6 in ethanol ($\phi_f = 0.78$) as standard.[45] Fluorescence lifetimes (τ_f) were measured with the stroboscopic technique employing a Photon Technology International (PTI) Strobe Master C-700 fluorometer (minimum measurable lifetime of 100 ps). The excitation source was a nanosecond flash lamp filled with a mixture of nitrogen and helium (30/70), and excitation was performed at 336 nm. Data were collected over 200 channels with a time base of 0.1 ns per channel. Fluorescence decays were analyzed using the software from PTI. All of the measurements were conducted at 25 °C in a thermostated cell.

Subpicosecond transient absorption and gain experiments were performed by the pump−probe technique with a white-light probe. The source is a non-mode-locked homemade dye laser described elsewhere.[46] It is driven by a single 10-Hz 6-ns Nd:YAG laser and delivers intense 600-fs pulses at 610 nm. This beam is used to produce a continuum of white light in a water cell, which is filtered and amplified in two separate, synchronous amplification chains. Two subpicosecond wavelengths were simultaneously generated at 570 nm (with rhodamine 6G as the gain medium) and at 427 nm (with stilbene 3) or 708 nm (with rhodamine 700). The 708-nm wavelength was frequency-doubled in a BBO crystal to produce a beam at 354 nm.

Pumping the sample was done with the 427-nm (free ligand) or 354-nm (calcium complex) beam, while the 570-nm beam generated the continuum of white light used as the probe. Pump−probe delays were adjusted by retarding the probe beam in a stepper-motor-driven optical delay line. The probe beam was split into a sample and a reference channel to compensate for energy and spectrum fluctuations. Pump and probe beams crossed on the sample, held in a 1-mm cuvette, at an angle of ~10°, and their polarizations were set at the magic angle. The sample solution (50 mL) was recirculated at room temperature to avoid significant photolysis during the time of the experiment; it was not deaerated. The transmitted beams were collected with 600-μm optical fibers and sent to a spectrograph (Jobin-Yvon 270M; grating = 100 grooves/mm; entrance slit = 64 μm). Spectra were recorded on a CCD camera (Princeton Instruments, 1024 × 128) and accumulated over 500 pump shots.

Time-resolved differential absorbance ($\Delta A = A - A_0$, where A is the excited sample absorbance and A_0 the steady-state absorbance) spectra shown here were calculated and corrected from group velocity dispersion on the probe beam (chirp) measured, in a separate experiment, by two-photon absorption in pure 1-chloronaphthalene. The experimental error on the differential absorbance measurements was estimated to be ±5 mOD and the time resolution to lie between 1 and 1.5 ps. After deconvolution, no lifetime shorter than 0.5 ps can nevertheless be measured by this setup.

Experiments on the free ligand were performed with a solution having a 0.55-OD/mm absorbance at the pump wavelength (427 nm), while a 0.63-OD/mm solution (at 354 nm) was used for the complex with calcium.

Results

Characterization of the Complexes by UV/Vis Absorption Spectroscopy. For the sake of clarity, some of the previously reported[39] spectroscopic properties of compound **A** in the presence of calcium perchlorate are recalled here. The UV/vis absorption spectrum of **A** in acetonitrile exhibits an intense band of charge-transfer nature[47−49] at 464 nm ($\epsilon = 68\,000\ M^{-1}\ cm^{-1}$), which decreases and shifts to the blue upon calcium addition. At high salt concentrations, a new absorption band appears at lower wavelengths, peaking at 375 nm (Figure 1).

These spectroscopic variations have been linked to the formation of three different complexes, AM, A_2M, and AM_2, of ligand to metal stoichiometry 1:1, 2:1, and 1:2, respectively. The corresponding association constants (K_1, K_2, and K_3), as well as their molar extinction coefficients, have been determined by a *global* analysis consisting in simultaneously fitting the

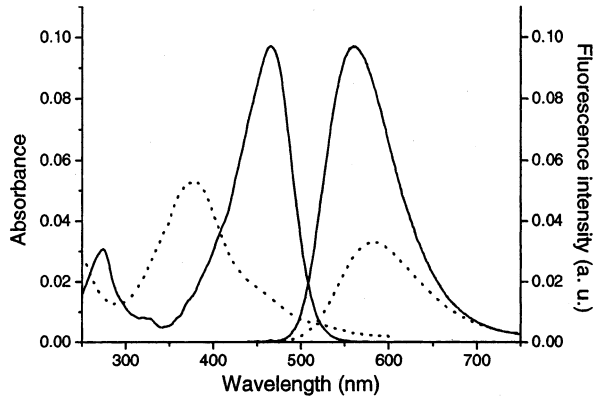

Figure 1. UV/vis absorption and fluorescence (excitation at 408 nm) spectra of a solution of **A** (1.42×10^{-6} M) in acetonitrile before (—) and after (···) addition of calcium perchlorate (1.75×10^{-2} M).

absorption changes versus calcium concentration at selected wavelengths, according to the following model:

$$A + M \rightleftharpoons AM \qquad K_1$$

$$AM + A \rightleftharpoons A_2M \qquad K_2$$

$$AM + M \rightleftharpoons AM_2 \qquad K_3$$

The calculated values were $K_1 = 6.2 \times 10^3$ M^{-1}, $K_2 = 8.4 \times 10^5$ M^{-1}, and $K_3 = 1.2 \times 10^3$ M^{-1}. This calculation also gave access to the proportion of each species versus calcium concentration. As the calcium concentration increases, the complexes appear in the order A_2M < AM < AM_2. The sandwich complex A_2M is principally formed at low calcium concentrations, whereas a mixture of AM and AM_2 complexes is found at higher salt concentrations.

From these values, we were able to calculate the conditions needed to prepare a solution in which AM_2 predominates and that complies with the requirements of the different experiments. For instance, for transient absorption spectroscopy, a mixture of 3.2×10^{-2} M Ca^{2+} and 2.1×10^{-4} M dye was used, which corresponds to a fraction of AM_2 complex greater than or equal to 97%.

The same data processing allowed the respective UV/vis absorption spectra to be reconstructed (Figure 2). In particular, it is interesting to note that the spectra of the AM and AM_2 complexes show an isosbestic point at 406 nm, and the spectra of the A and AM_2 intersect at 408 nm.

Steady-State Fluorescence. In the absence of salt, the emission spectrum of **A** (1.42×10^{-6} M) in acetonitrile exhibits an intense long-wavelength band with a maximum situated at 562 nm and a fluorescence quantum yield (ϕ_f) of 0.14.[42] The addition of a calcium concentration (1.75×10^{-2} M) such that the dicomplexed ligand AM_2 is the predominant species (95.4% AM_2; 4.56% AM, 0.002% A_2M, and 0.04% A) results in a drop of the fluorescence intensity ($\phi_f = 0.057$), accompanied by a significant red shift of the emission band ($\lambda_{em} = 583$ nm). The emission spectra of the AM_2-rich solution and of the free ligand **A** are depicted in Figure 1 for an excitation wavelength (408 nm) chosen so that their intensities of fluorescence may be directly compared.

The emission spectrum of the AM_2-rich solution is 20 nm red-shifted from that of the free ligand. That means that it probably cannot be accounted for by some kind of loose complex, that is, a species in which the two nitrogen−calcium bonds are disrupted and that would be comparable to **A**. Moreover, the π-electron system of the dicomplex AM_2 can be

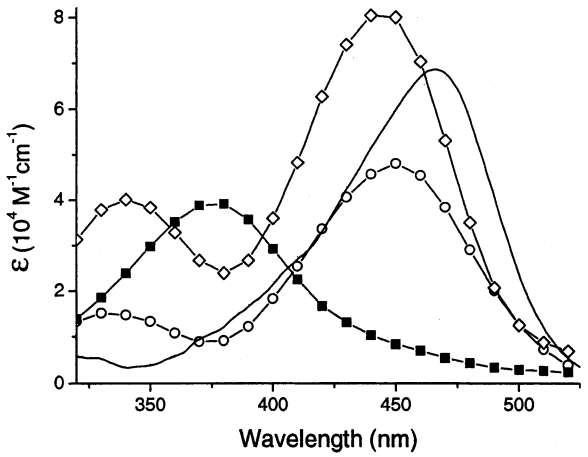

Figure 2. UV/vis Absorption spectrum of compound **A** (—) and reconstructed absorption spectra of the three ligand/metal complexes, AM (○), A_2M (◇), and AM_2 (■), formed with Ca^{2+} in acetonitrile. The reconstructed spectra derive from the calculation of the association constants by a simultaneous fit of titration curves at 21 different wavelengths.[39]

compared to that of diphenylpentadienone, which has been reported not be fluorescent in solution at room temperature.[50,51]

One could imagine that the fluorescence observed after excitation of the AM_2-rich solution might be due to the AM complex present in the solution. As a matter of fact, 2,5-[4-(diethylaminophenyl)phenyl]methylene]cyclopentanone has also a red-shifted emission (598 nm) and a weak fluorescence quantum yield (0.025) in acetonitrile. Assuming, on one hand, that the electronic structure of the phenyl end group is similar to that of the azacrown filled with a cation and, on the other hand, that the diethylaminophenyl end group is similar to an empty azacrown, this compound may be considered as a model compound for AM, provided the latter does not liberate its cation in the excited state. However, under these experimental conditions, the amount of AM complex in the AM_2-rich solution would be too weak to account for the fluorescence intensity observed.

An alternative proposal would be to consider an interaction between the cation and the unsaturated core of the ligand. It was shown that such an interaction occurs for bis-crown-diphenylpentadienone (the flexible analogue of **A)** in the presence of divalent cations and is responsible for a red shift of the fluorescence spectrum.[38] However, this latter species is formed in much smaller proportions than the AM complex where the crown cavity is complexed. Consequently, it appears clearly that the distribution of the species in the ground state cannot explain the fluorescence spectrum observed for the AM_2-rich solution. This suggests that the deactivation pathway of AM_2 involves an excited-state reaction, which has been investigated here by ultrafast spectroscopy.

Fluorescence Lifetime Measurements. The fluorescence decays were measured at different wavelengths (575 and 600 nm) for a solution of calcium-free **A** and for a solution predominantly containing the AM_2 complex. For the free ligand, the fluorescence decay was suitably fitted with a single exponential of 0.8 ns, a lifetime close to that previously measured for bis-crown-diphenylpentadienone.[38] The fluorescence decay of the AM_2-rich solution was found to be monoexponential with a lifetime of 1.1 ns. This value is significantly longer than that of **A**, supporting previous assumptions that the AM_2 excited-state relaxation does not involve a simple concerted decomplexation process of the two ions. To interpret the fluorescence spectra, we invoked in the previous

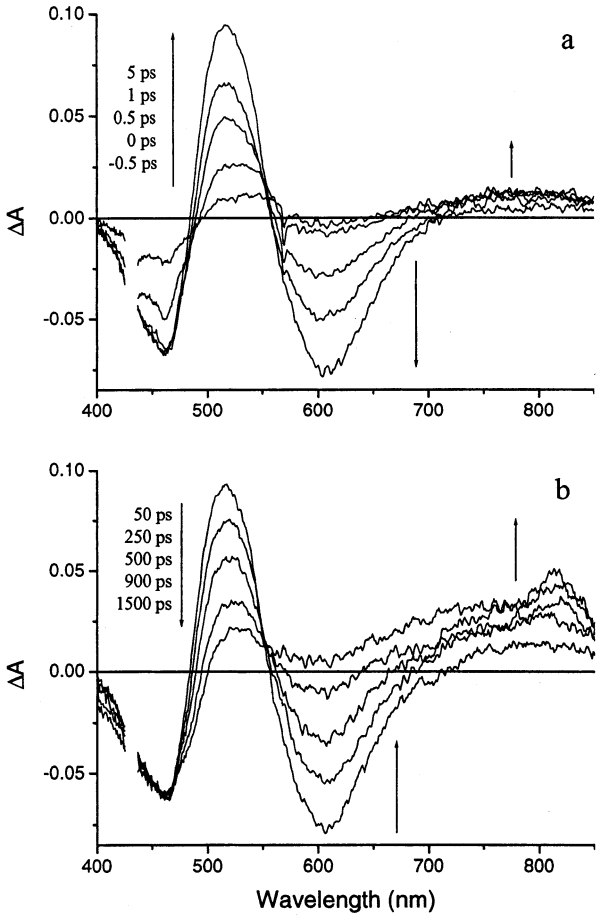

Figure 3. Differential absorbance $\Delta A(\lambda,t)$ of **A** (1.47×10^{-4} M) in acetonitrile (a) between −0.5 and 5 ps and (b) between 50 and 1500 ps after excitation with a 0.6-ps pulse at 427 nm. The transient spectra are corrected from the chirp.

section the possible detection of the AM fluorescence, the lifetime of which is not known. One may infer that it could lie between 200 and 300 ps, according to measurements performed on the flexible analogue[52] and on 2,5-[4-(diethylaminophenyl)-phenyl]methylene]cyclopentanone (this work) in acetonitrile. Several interpretations can be found for the absence of such a short component: the excited state of the so-called model compound might actually not be a good model for AM* or else AM* might not be present in the solution or its contribution to the total fluorescence might be too weak.

Subpicosecond Pump−Probe Experiments. *Time-Resolved Differential Spectra of the Free Ligand Solution.* Figure 3 shows the differential absorbance spectra (ΔA) of a free ligand solution in acetonitrile (1.47×10^{-4} M) in the 400−850 nm spectral range recorded for pump−probe delays going from −0.5 to 1500 ps after excitation at 427 nm. A broad negative band characterizing the bleaching of the ground-state absorption ($\Delta A < 0$, $A_0 > 0$), situated between 400 and 485 nm, is observed for all of the recorded pump−probe delays. During the pump−probe overlap, the spectra display a broad transient absorption band ($\Delta A > 0$) in the 485−560 nm range with a maximum situated at 528 nm. In the first 5 ps, this band further grows (Figure 3a), its maximum shifts to the blue (518 nm), and a net gain band ($\Delta A < 0$, $A_0 = 0$) appears in the 560−700 nm range, peaking at 605 nm. A broad absorption band of weak intensity situated between 700 and 850 nm appears within the pump−probe overlap and does not show any noticeable increase in the following few picoseconds. From 5 to 50 ps, the transient spectra do not evolve any more. At longer delays, between 50 and 1500 ps (Figure 3b), the intensity of the absorption band initially situated at 518 nm decreases, and the band progressively shifts to the red, finally peaking near 530 nm. At the same time, the gain band decays and the redmost absorption band rises in the 600−850 nm range, growing a narrow peak at 815 nm. An important bleaching is still observed at 1500 ps.

To explain the shift of the blue transient absorption band (485−560 nm) occurring within the pump−probe overlap, several phenomena can be invoked. Solvent relaxation must be discarded because the experiments were performed in acetonitrile, a solvent known to exhibit a very fast reorganization time (260 fs).[53] Another possibility could be that compound **A** was excited with an energy excess estimated around 3800 cm^{-1} (roughly situating the 0−0 transition around the crossing point of the normalized steady-state absorption and fluorescence spectra). Vibrational cooling is then expected although it may not be observable because the number of normal modes over which the energy excess can redistribute is extremely large (306). An alternative explanation may also be sought in the charge-transfer nature of the fluorescing state of the ligand, revealed by a positive solvatochromism of its diethylamino parent compound.[49] As in the case of the merocyanine dye DCM,[54] it could be hypothesized that the locally excited state (LE) suddenly reached after the excitation pulse is less polar than the charge-transfer fluorescing state (CT) and that our observation reflects the ultrafast formation of the CT state from the LE state.

As for the slow rise of the transient absorption band on the red edge of the spectra, it is reasonable to assign it to the triplet-state formation. The triplet absorption spectrum of the parent compound, **A** substituted by two diethylamino groups instead of azacrowns, was reported by Barnabas et al.[47] Its shape is consistent with that of the transient spectrum recorded for the longest delay time in our experiments. In particular, the triplet absorption maximum was reported to be 820 nm in acetonitrile, which agrees well with the peak that we observed at 815 nm.

It is interesting to note that the time-resolved differential spectra measured above 50 ps considerably differ from those observed by DeVoe et al. on the bis-(dimethylamino-benzylidene)acetone derivative, the diethylamino flexible analogue of compound **A**.[55] For this compound, no gain bands have been detected in the transient spectra, even at the shortest time recorded after excitation (50 ps). The authors proposed that the initially excited state rapidly converts, by twisting of the vinylic double bond, to a phantom state. It is nevertheless not clear to us why the presence of an ethylene bridge in compound **A** could impede such an isomerization and allow a gain band. Possibly the presence of rotational isomers, which have not been taken into account in DeVoe's photophysical study, could provide an alternative explanation for the deactivation pathway of the flexible compound.

Time-Resolved Differential Spectra of the AM_2-Rich Complex Solution. Figure 4 shows time-resolved absorption spectra of an acetonitrile solution mainly containing the AM_2 complex, recorded after excitation at 354 nm in the 360−850 nm spectral range. Immediately after excitation, a strong bleaching band appears under 400 nm and remains up to the longest delay time recorded here (1500 ps). Within the pump−probe overlap (Figure 4a), a broad absorption band showing two maxima at 428 and 514 nm, a net gain band around 610 nm, and a broad absorption band in the 700−850 nm region appear. Within 6 ps after excitation, the 428 nm absorption band drastically decreases while that at 514 nm still grows as also slightly does

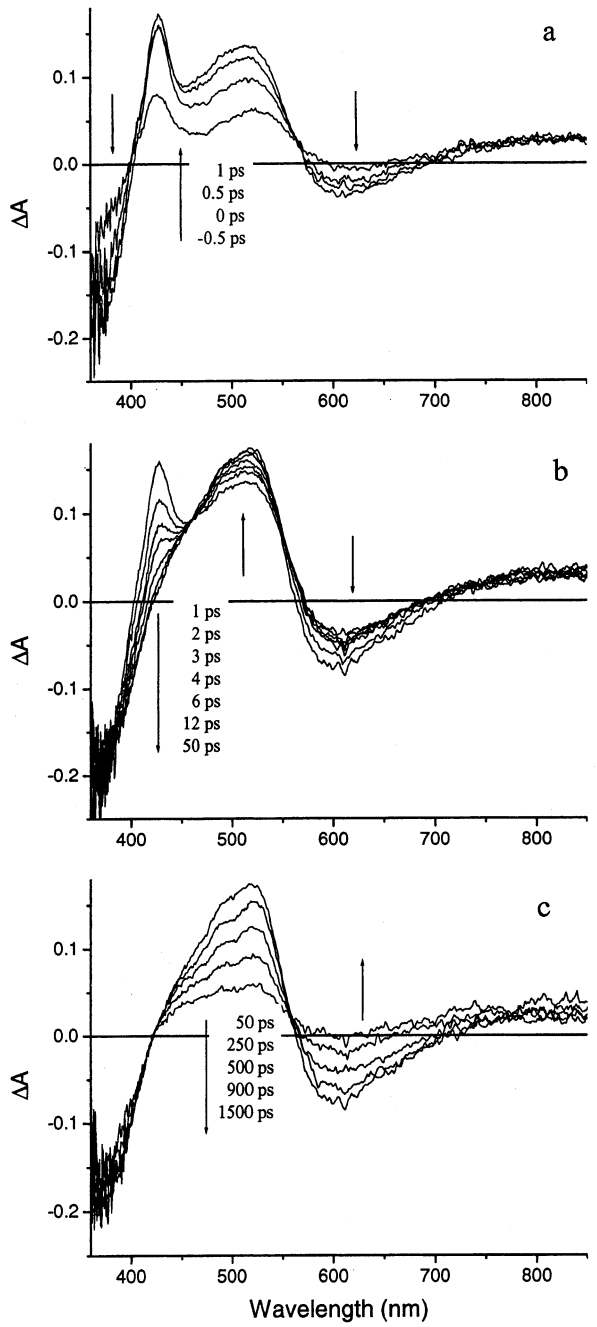

Figure 4. Differential absorbance $\Delta A(\lambda,t)$ of **A** (2.1×10^{-4} M) in acetonitrile in the presence of Ca^{2+} (3.2×10^{-2} M) (a) within the pump−probe overlap, (b) between 1 and 50 ps, and (c) between 50 and 1500 ps after excitation with a 0.6-ps pulse at 354 nm. The transient spectra are corrected from the chirp.

the gain band (Figure 4b). These changes occur on either sides of two temporary isosbestic points (ΔA = constant) seen at 460 and 557 nm. At the same time, the long-wavelength absorption band remains unchanged. Between 6 and 50 ps, the major changes are observed in the gain band, which keeps on increasing. The absorption band initially situated at 514 nm slightly shifts to 518 nm without noticeable increase in optical density, and the long-wavelength absorption band remains constant. For delay times between 50 and 1500 ps, the broad absorption band centered at 518 nm decreases and flattens, the gain band completely disappears, and the long-wavelength absorption band rises for finally extending from 640 to over 850 nm. As in the case of the free ligand, this slow dynamics is very likely to be due to the formation of a triplet state.

SCHEME 2: Kinetic Model of the Deactivation Pathways of A

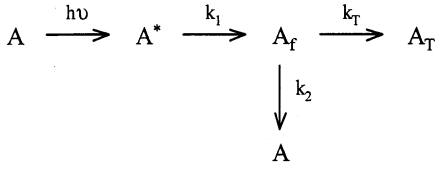

The most striking feature observed in the differential absorbance spectra of the AM_2 complex at early times is the collapse of the transient absorption band situated at 428 nm in favor of the 514 nm absorption band, occurring in a few picoseconds. The presence of clear temporary isosbestic points suggests a precursor−successor relationship between two states or species. A third species is then very likely to appear, between about 10 and 50 ps, because the blue transient absorption band is found not to evolve while the gain band grows. At this point, it is still premature to discuss the nature of those intermediate species until a more precise analysis of the data has been done (see next section).

It is nevertheless interesting to note that the transient spectra of AM_2 differ somewhat from those of the free ligand at long times, particularly by the absence of the peak at 815 nm in the triplet absorption region. It seems then that the last species reached at 1500 ps cannot be related to the free ligand, which means that the ejection of the two cations does not occur. This hypothesis supports the conclusions of the steady-state fluorescence study.

Data Analysis

Kinetic Model of the Free Ligand. We performed a global analysis (see Appendix for details of the procedure) of the transient absorption spectra of the free ligand. Fitting of the kinetic data was simultaneously performed at 21 wavelengths evenly chosen between 400 and 800 nm using a kinetic model involving three excited states: A*, the initially pumped state, the fluorescing state A_f, and a triplet state A_T, linked as depicted in Scheme 2.

Attempts to omit one of the three states were unsuccessful; Scheme 2 should be considered as the minimal model able to satisfactorily fit our data. Figure 5a shows the adjustments obtained at selected wavelengths in the bleaching (460 nm), main transient absorption (520 nm), stimulated emission (600 nm), and far-red absorption (800 nm) bands. Good fits were obtained at all wavelengths for all pump−probe delays.

The optimized rate constants are $k_1 = 7.5 \times 10^{11}$ s^{-1}, $k_2 = 7.2 \times 10^8$ s^{-1}, and $k_T = 5.5 \times 10^8$ s^{-1}, corresponding to the A* → A_f ultrafast dynamics, the (radiative and nonradiative) ground-state recovery from A_f, and the intersystem crossing, respectively. The fluorescence lifetime ($\tau_f = (k_2 + k_T)^{-1}$) recalculated from these values is 0.79 ns, in very good agreement with the fluorescence lifetime of 0.8 ns that we measured independently (see Fluorescence Lifetime Measurements). On the other hand, the triplet yield ($\phi_T = k_T(k_T + k_2)^{-1}$) is found to be 0.43, which is in reasonable agreement with the value of 0.36 reported by Barnabas et al. for the bis(diethylamino) parent compound of **A**.[47] Figure 5b shows the generalized absorption spectra (ϵ_g = absorption coefficient minus stimulated-emission coefficient, see Fitting the Data in the Appendix) of the three states involved in the relaxation of **A**.

Kinetic Model of the AM_2 Complex. The time-resolved spectra of AM_2 were fitted at 20 wavelengths ranging from 390 to 660 nm. Good results were attained with kinetic Scheme 3,

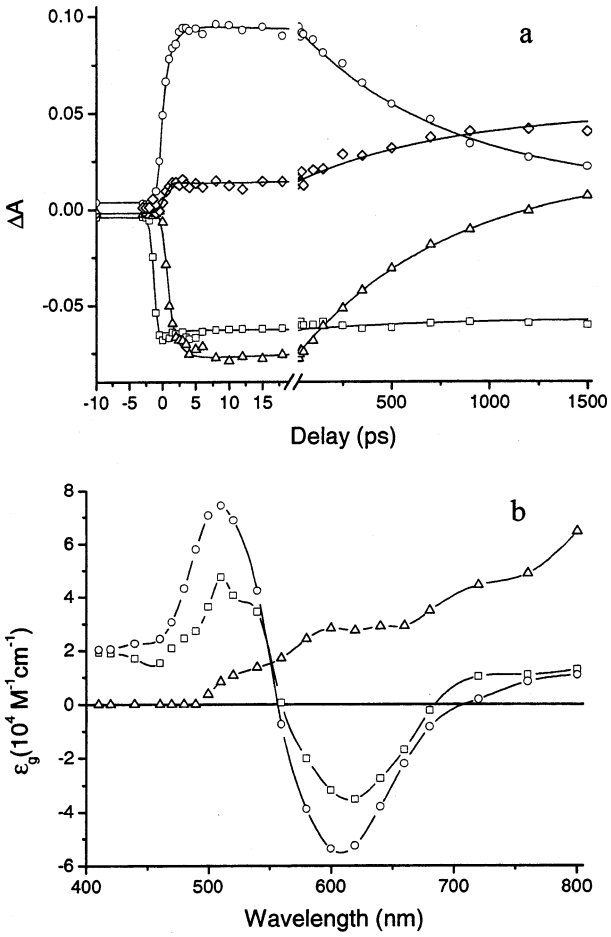

Figure 5. Kinetic modeling of the time-resolved spectra of compound **A** (1.47×10^{-4} M) in acetonitrile: (a) fits of the differential absorbance kinetics data $\Delta A(\lambda,t)$ at selected wavelengths, $\lambda_{obs} = 460$ nm (□), $\lambda_{obs} = 520$ nm (○), $\lambda_{obs} = 600$ nm (△), and $\lambda_{obs} = 800$ nm (◇); (b) calculated transient spectra (ϵ_g = absorption coefficient minus stimulated-emission coefficient, see Fitting the Data in the Appendix) of the A* (□), A_f (○), and A_T (△) states (solid lines are smooth curves joining the calculated points to help visualizing the spectra).

SCHEME 3: Kinetic Model of the Deactivation Pathways of AM_2

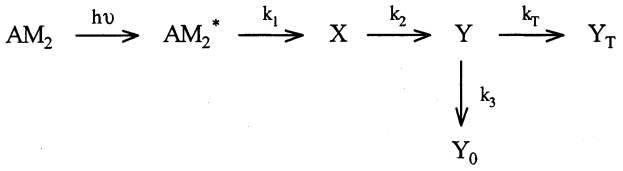

which involves one more step than that for the free ligand. Once again, different models were tested but this one was preferred as being the simplest to satisfactorily account for the dynamical behavior of the complex.

In Scheme 3, AM_2* stands for the initially pumped Franck−Condon state, X and Y are two cascading excited states, the last one relaxing both to a ground-state Y_0 and a triplet state Y_T. In a first step, the absorption coefficients of species Y_0 were set as adjustable parameters, and the reconstructed spectrum resembled very much the ground-state absorption of the AM complex, depicted in Figure 2. This close similarity allowed us to assign Y_0 to species AM. In a second step, we fixed the Y_0 absorption coefficients to the ones of the AM complex, to further constrain the fitting system and obtain more reliable results. Excellent fits were obtained, as examplified in Figure 6a, with only slight deviations with respect to the first adjustment. The

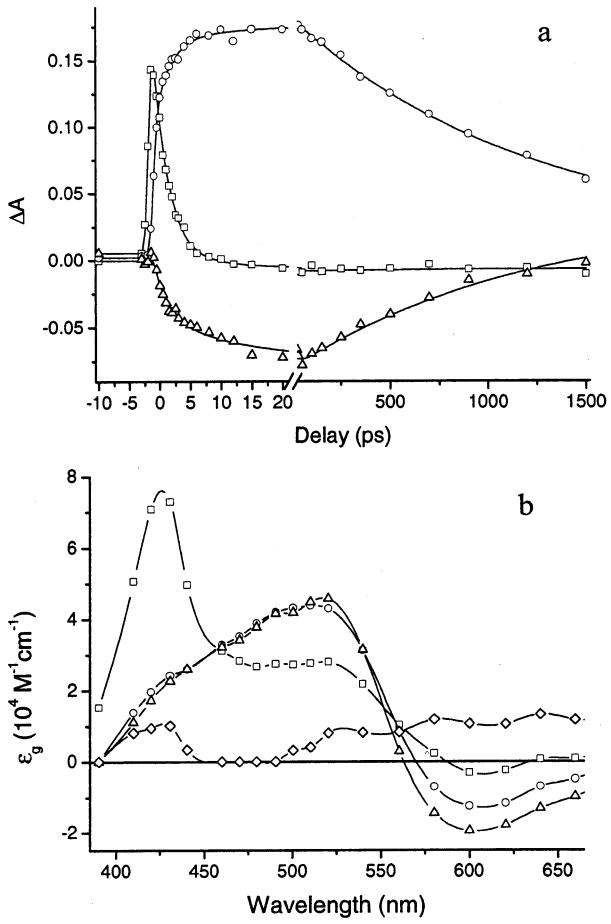

Figure 6. Kinetic modeling of the time-resolved spectra of the AM_2 complex in acetonitrile: (a) fits of the differential absorbance kinetics data $\Delta A(\lambda,t)$ at selected wavelengths, $\lambda_{obs} = 420$ nm (□), $\lambda_{obs} = 520$ nm (○), and $\lambda_{obs} = 600$ nm (△); (b) calculated transient spectra (ϵ_g = absorption coefficient minus stimulated-emission coefficient, see Fitting the Data in the Appendix) of the AM_2* (□), X (○), Y (△), and Y_T (◇) states (solid lines are smooth curves joining the calculated points to help visualizing the spectra).

optimized rate constants were then $k_1 = 4 \times 10^{11}$ s^{-1}, $k_2 = 5.8 \times 10^{10}$ s^{-1}, $k_3 = 5.4 \times 10^8$ s^{-1}, and $k_T = 2.8 \times 10^8$ s^{-1}. Here too, the fluorescence lifetime ($\tau_f = (k_3 + k_T)^{-1} = 1.2$ ns) recalculated from these values agrees well with the direct experimental measurement (1.1 ns, see Fluorescence Lifetime Measurements). The absorption spectra of the various extracted species are presented in Figure 6b. Before going into the discussion on the details of the excited mechanism and on a possible attribution of the X and Y states, it seems necessary to comment on these spectra. One must note that an absorption shoulder and a small gain peak are found for the AM_2* precursor exactly at the spectral position of the absorption and gain bands of the successor X. This finding may be inherent to the global analysis procedure that we used. As a matter of fact, one did not take into account any molecular mechanism with non-exponential or multiexponential kinetics such as those met on very short times when the excited population propagates along a barrierless or quasi-barrierless potential. The initial reaction $AM_2^* \rightarrow X$ might better be described by such a reaction, in which part of the X population would be produced in the femtosecond regime. Our monomolecular description would only evidence the slower part of the process ($k_1 = 4 \times 10^{11}$ s^{-1}), accessible to our temporal resolution. Keeping this in mind, one may however discuss the different step of the excited mechanism.

Discussion

Considering the results of the kinetic analysis for the free ligand with Scheme 2, it is striking to note the similarity of the spectra of states A_f and A* (Figure 5b). The spectrum of A_f is nevertheless more intense and shows an unstructured absorption band together with a slightly blue-shifted emission. This last trend does not support a description of the initial fast $A^* \rightarrow A_f$ reaction as an excited-state charge-transfer mechanism. This would, on the contrary, induce a red shift of the emission. We thus prefer the vibrational cooling hypothesis in which A* represents a hot excited state and A_f the thermalized state, although the explanation is not totally convincing because no narrowing of the bands could be observed. In any case, the actual mechanism responsible for the ultrafast kinetics of **A** is not crucial to the argument of the present work. What really matters here is the accurate description that we obtained of the photophysical behavior of the free ligand and that will be compared to that of the AM_2 complex.

From our analysis in the last section, it appears that the ground-state AM monocomplex is likely one of the products of the AM_2 excited-state dynamics. This monocomplex is expected to rapidly convert into the initial AM_2 dicomplex by ground-state geminate recombination. Such a recombination is not observed in our experiments, even for the longest time recorded after excitation. This means that one of the two initially bound calcium cations is ejected sufficiently far away from the crown in the excited state so that its ground-state geminate recombination does not take place. In brief, one of the nitrogen−cation bonds is broken and calcium is released into the bulk.

It is now necessary to discuss how the AM complex could be formed, that is, to identify the Y then the X species of Scheme 3. Bearing in mind that the AM complex could come from a fast ground-state geminate recombination, which cannot be observed because of its high rate, the molecule could have undergone in the Y excited state either one or two disruptions of the nitrogen−calcium bonds. The excited-state Y precursor could then be a "tight" AM* complex or else a loose (A···M)* complex. The spectrum of the species showing a bis bond disruption is expected to look like that of the A_f state of the free ligand. Except for AM_2*, the spectra obtained after excitation of the AM_2 complex (Figure 6b) resemble somewhat that of the A_f state (Figure 5b) but considerably differ in the relative intensities of the gain and absorption bands. One then proposes to assign the Y precursor state to the AM* species, in which only one of the nitrogen−calcium bonds is broken. One already noted that its fluorescence lifetime of 1.1 ns considerably differs from the one that we measured for 2,5-[4-(diethylaminophenyl)phenyl]methylene]cyclopentanone (about 0.2 ns in acetonitrile), a so-called AM model compound (see Steady-State Fluorescence and Fluorescence Lifetime Measurements), but one cannot claim that the similarity in their ground-state structure still holds in the excited state. In any case, the present assignment may only be considered as tentative although it seems to us the most reasonable at present. Alternatively, a red-shifted emission with a reduced quantum yield could also be accounted for by species—free ligand, "tight", or loose complexes—in which the cation interacts with the carbonyl group of the molecule. Such an interaction can be considered as similar to what is observed in hydrogen-bond-donating solvents for compounds belonging to this chalcone family.[56−59] From our own work in protic solvents (unpublished results), we know that this interaction is expected to induce an enhancement of the nonradiative deactivation constant, which is in contradiction with the increased fluorescence lifetime observed here. This very argument holds also true to rule out a hypothetical role played by water (originating from the hydrated calcium perchlorate used), which could bind to the chromophore by hydrogen bond. This effect would identically promote short-lived species. A hypothetical explanation for the long lifetime of AM* compared to that known for the compound proposed as a possible model in acetonitrile might thus be found in possible environmental effects due to the addition of cations to the neat solvent.

If we now look at the beginning of the exited-state dynamics, we see that the initially excited state, that is, AM_2* according to our notation, disappears in a few picoseconds to produce a strongly red-shifted species (X). From the preceding discussion, it is reasonable to ascribe this reaction to the disruption of a nitrogen−calcium bond in one of the crowns. It may be noticed that the rate constant of this bond disruption is of the same order of magnitude as those reported for DCM-crown[16] and DCS-crown[18] complexed with calcium. The question is then to know whether, in state X, the cation is ejected outside of the crown cavity or whether it remains inside. A good hint is provided by the close spectral similitude of species X and Y (AM*) (see Figure 6b). Most of the difference lies in the intensity of the stimulated emission band. One can think that this modest but still significant difference does not signal a real change of the chromophore state but rather a change of its environment. On the other hand, the stimulated emission band is still more intense for the free ligand (Figure 5b), that is, when the ions are absent. We propose that the stimulated emission enhancement observed during the ca. 20 ps that it takes to go from X to AM* reflects the actual moving of the cation out of the crown. According to that view, X stands then for an excited species in which one cation bond has been disrupted, leaving the cation inside of the crown, while the other cation remains tightly bound to the other crown. Such a state can symbolically be noted as (M···AM)*.

Conclusion

The steady-state spectroscopic properties of 2,5-[bis-[4*N*-(aza-15-crown-5)phenyl]methylene]cyclopentanone (**A**) in acetonitrile are greatly affected by the presence of calcium cation. Upon complexation of the two crowns, the UV/vis absorption spectrum drastically shifts to the blue whereas the fluorescence spectrum undergoes a large red shift. This unusual behavior is particularly attractive for wavelength-ratiometric sensing. On the basis of fluorescence data, a photophysical mechanism probably involving an excited-state decomplexation was considered. The free ligand **A** and its calcium dicomplex AM_2 were investigated by time-resolved absorption and gain spectroscopy, in the picosecond regime, and their spectra were compared. The suspected excited-state reactivity of AM_2 was confirmed by very large spectral modifications recorded just a few picoseconds after excitation. Fitting the spectrodynamic data of AM_2 with a global analysis procedure, we tentatively propose a detailed molecular model that satisfactorily accounts for the observed behavior. Our scheme includes the following steps: a disruption of one of the nitrogen−cation bonds that would take place at rate constant of 4×10^{11} s^{-1}, followed by the diffusion of the cation out of the crown at a rate constant of 5.8×10^{10} s^{-1}. The produced excited AM* complex would subsequently relax to both its ground state (AM) and its triplet state in the nanosecond regime. A long-lived and reversible photorelease of a calcium cation is thus here proposed upon irradiation of AM_2. In addition to its suitability for cation recognition, compound **A** may then also provide an interesting way to produce temporally and spatially controlled jumps of the intracellular concentration of certain biologically relevant metal cations.

Compared to other cation−azacrown photodisruptive systems reported so far, AM_2 displays especially large transient and steady-state spectroscopic features. This might be linked to the particular D−A−D pattern of the π system, which confirms the interest of such structures for the design of efficient fluoroionophores.

Appendix: Modeling and Fitting of the Kinetics Data

Kinetic Model. The transient spectra of the free ligand (**A**) and of the calcium dicomplex (AM_2) were analyzed according to kinetic models that describe how the excitation pulse pumps part of the ground-state population S_0 to the Franck−Condon state and how this excited population spontaneously evolves through successive transient (excited or ground) states by monomolecular reactions. As an example, we will examine here the case of species AM_2 of which the photophysical behavior is described by kinetic Scheme 3 (Kinetic Model of the AM_2 Complex).

For the sake of simplicity, no propagation of the pump or probe beams was taken into account. The sample was considered as thicknessless and the beams transversely homogeneous. The differential equation describing the pumping process is written as follows:

$$\mathrm{d[AM_2]}/\mathrm{d}t = -I_0 J(t)(1 - 10^{-\mathrm{Abs_{tot}}(t)})\frac{\mathrm{Abs_{AM_2}}(t)}{\mathrm{Abs_{tot}}(t)} \quad (1)$$

where $\mathrm{Abs_{tot}}(t)$ is the time-dependent absorbance of the sample at the excitation wavelength and $\mathrm{Abs_{AM_2}}(t)$ is the part of this absorbance due to the AM_2 ground-state species. I_0 (in M^{-1}) is the number of incident photons per excitation pulse in the excited volume, assumed to be a homogeneous cylinder. $J(t)$ (in s^{-1}) is the normalized excitation pulse shape, approximated by a hyperbolic secant square function of 0.6 ps full width at half-maximum.

The time-dependent evolution of the successive excited-state populations is determined by the following differential equations:

$$\mathrm{d[AM_2{}^*]}/\mathrm{d}t = I_0 J(t)(1 - 10^{-\mathrm{Abs_{tot}}(t)})\frac{\mathrm{Abs_{AM_2}}(t)}{\mathrm{Abs_{tot}}(t)} - k_1[\mathrm{AM_2{}^*}] \quad (2)$$

$$\mathrm{d[X]}/\mathrm{d}t = k_1[\mathrm{AM_2{}^*}] - k_2[\mathrm{X}] \quad (3)$$

$$\mathrm{d[Y]}/\mathrm{d}t = k_2[\mathrm{X}] - (k_\mathrm{T} + k_3)[\mathrm{Y}] \quad (4)$$

$$\mathrm{d[Y_0]}/\mathrm{d}t = k_3[\mathrm{Y}] \quad (5)$$

$$\mathrm{d[Y_T]}/\mathrm{d}t = k_\mathrm{T}[\mathrm{Y}] \quad (6)$$

Fitting the Data. The differential equations system 1−6 was numerically integrated using a semiimplicit Runge−Kutta integrator.[60] The calculated concentration kinetics of the fast species (steps 2−4) were then convoluted up to 150 ps by the probe beam temporal profile. The probe profile was assumed to have a hyperbolic secant square shape, the width of which was introduced as an adjustable parameter for each observation wavelength. A wavelength-dependent time shift was also introduced as an adjustable parameter in each probe profile to take into account the fact that the various spectral components do not reach the sample at the same time because of group velocity dispersion (chirp effect). These concentrations were then used to calculate the differential absorbance $\Delta A(\lambda,t)$ defined as follows:

$$\Delta A(\lambda,t) = A(\lambda,t) - A_0(\lambda) = \sum_i (\epsilon_{\mathrm{g}i}(\lambda) - \epsilon_\mathrm{a}(\lambda))C_i(t)l \quad (7)$$

where A_0 is the steady-state absorbance of the sample, $A(t)$ is the absorbance of the pumped sample at time t, and l is the optical path length. The sum is taken over all "transient" species, that is, all species different from the initial molecule in its ground-state. In our example, this list includes AM_2*, X, Y, Y_0, and Y_T. C_i is the concentration of transient species i, ϵ_a is the ground-state absorption coefficient of the initial molecule (AM_2 here), and $\epsilon_{\mathrm{g}i}$ the "generalized" absorption coefficient (ϵ_g = absorption coefficient minus stimulated-emission coefficient) of transient species i.

A nonlinear least-squares minimization procedure was then applied to simultaneously fit the kinetic traces at about 20 wavelengths, according to the Powel algorithm.[61] It must be noted that the fluence parameter I_0 allows us to access through eq 2 to absolute excited-state concentrations. This is what permits us to extract absolute (generalized) absorption coefficient spectra. Unfortunately, I_0 is not known experimentally with enough precision, so this number was left as an adjustable parameter that we optimized by imposing a particular constraint on the transient spectra. Because choosing I_0 determines the initial ground-state AM_2 depletion, incorrectly setting it produces an undercompensation or an overcompensation of the bleaching signal. Our constraint was then to obtain "bleaching-free" transient spectra, which was checked by visual inspection. Although reasonable, this condition is certainly arbitrary to a certain extent, but the impact of an error on I_0 is negligible on the shape of the spectra above 450 nm, where the ground-state AM_2 absorption disappears.

References and Notes

(1) *Fluorescent Chemosensors for Ion and Molecule Recognition*; Czarnik, A. W., Ed.; ACS Symposium Series 538: American Chemical Society, Washington, DC, 1992.

(2) *Topics in Fluorescence Spectroscopy. Probe Design and Chemical Sensing*; Lakowicz, J. R., Ed.; Plenum Press: New York, 1994; Vol. 4.

(3) *Chemosensors of Ion and Molecule Recognition*; Desvergne, J. P., Czarnik, A. W., Eds.; Nato ASI Series, Vol. 492; Kluwer Academic Publishers: Dordrecht, Netherlands, 1997.

(4) Rettig, W.; Rurack, K.; Scepan, M. In *New Trends in Fluorescence Spectroscopy: Application to Chemical and Life Sciences*; Valeur, B., Brochon, J.-C., Eds.; Springer-Verlag: Berlin, 2001; p 125.

(5) Valeur, B.; Leray, I. In *New Trends in Fluorescence Spectroscopy: Application to Chemical and Life Sciences*; Valeur, B., Brochon, J.-C., Eds.; Springer-Verlag: Berlin, 2001; p 187.

(6) de Silva, A. P.; Gunaratne, H. Q. N.; Gunnlaugsson, T.; Huxley, A. J. M.; McCoy, C. P.; Rademacher, J. T.; Rice, T. E. *Chem. Rev.* **1997**, *97*, 1515.

(7) Rurack, K. *Spectrochim. Acta, Part A* **2001**, *57*, 2161.

(8) Valeur, B. In *Topics in Fluorescence Spectroscopy. Probe Design and Chemical Sensing*; Lakowicz, J. R., Ed.; Plenum Press: New York, 1994; p 21.

(9) Bourson, J.; Valeur, B. *J. Phys. Chem.* **1989**, *93*, 3871.

(10) Létard, J.-F.; Lapouyade, R.; Rettig, W. *Pure Appl. Chem.* **1993**, *65*, 1705.

(11) Druzhinin, S. I.; Rusalov, M. V.; Uzhinov, B. M.; Gromov, S. P.; Sergeev, S. A.; Alfimov, M. V. *J. Fluoresc.* **1999**, *9*, 33.

(12) Rurack, K.; Bricks, J. L.; Reck, G.; Radeglia, R.; Resch-Genger, U. *J. Phys. Chem. A* **2000**, *104*, 3087.

(13) Jonker, S. A.; Ariese, F.; Verhoeven, J. W. *Recl. Trav. Chim. Pays-Bas* **1989**, *108*, 109.

(14) Martin, M. M.; Plaza, P.; Dai Hung, N.; Meyer, Y. H.; Bourson, J.; Valeur, B. *Chem. Phys. Lett.* **1993**, *202*, 425.

(15) Martin, M. M.; Plaza, P.; Meyer, Y. H.; Bégin, L.; Bourson, J.; Valeur, B. *J. Fluoresc.* **1994**, *4*, 271.

(16) Martin, M. M.; Plaza, P.; Meyer, Y. H.; Badaoui, F.; Bourson, J.; Lefèvre, J.-P.; Valeur, B. *J. Phys. Chem.* **1996**, *100*, 6879.

(17) Dumon, P.; Jonusauskas, G.; Dupuy, F.; Pée, P.; Rullière, C.; Létard, J.-F.; Lapouyade, R. *J. Phys. Chem.* **1994**, *98*, 10391.
(18) Mathevet, R.; Jonusauskas, G.; Rullière, C.; Létard, J.-F.; Lapouyade, R. *J. Phys. Chem.* **1995**, *99*, 15709.
(19) Jonusauskas, G.; Lapouyade, R.; Delmond, S.; Létard, J. F.; Rullière, C. *J. Chem. Phys.* **1996**, *93*, 1670.
(20) Plaza, P.; Leray, I.; Changenet-Barret, P.; Martin, M. M.; Valeur, B. *ChemPhysChem* **2002**, *3*, 668.
(21) Berridge, M. J. *Nature* **1993**, *361*, 315.
(22) Tsien, R. Y. In *Fluorescent Chemosensors for Ion and Molecule Recognition*; Czarnik, A. W., Ed.; ACS Symposium Series 538: American Chemical Society: Washington, DC, 1992; p 130.
(23) Masilamani, D.; Lucas, M. E. In *Fluorescent Chemosensors for Ion and Molecule Recognition*; Czarnik, A. W., Ed.; ACS Symposium Series 538: American Chemical Society: Washington, DC, 1992; p 162.
(24) Rajesh, C. S.; Givens, R. S.; Wirz, J. *J. Am. Chem. Soc.* **2000**, *122*, 611.
(25) Granjon, T.; Vacheron, M.-J.; Vial, C.; Buchet, R. *Biochemistry* **2001**, *40*, 2988.
(26) Boittin, F.-X.; Coussin, F.; Morel, J.-L.; Halet, G.; Macrez, N.; Mironneau, J. *Biochem. J.* **2000**, *349*, 323.
(27) Albota, M.; Beljonne, D.; Brédas, J.-L.; Ehrlich, J. E.; Fu, J.-Y.; Heikal, A. A.; Hess, S. E.; Kogej, T.; Levin, M. D.; Marder, S. R.; McCord-Maughon, D.; Perry, J. W.; Röckel, H.; Rumi, M.; Subramaniam, G.; Webb, W. W.; Wu, X.-L.; Xu, C. *Science* **1998**, *281*, 1653.
(28) Hahn, S.; Kim, D.; Cho, M. *J. Phys. Chem. B* **1999**, *103*, 8221.
(29) Ventelon, L.; Moreaux, L.; Mertz, J.; Blanchard-Desce, M. *Synth. Met.* **2002**, *127*, 17.
(30) Barzoukas, M.; Blanchard-Desce, M. *J. Chem. Phys.* **2000**, *113*, 3951.
(31) Ventelon, L.; Moreaux, L.; Mertz, J.; Blanchard-Desce, M. *Chem. Commun.* **1999**, 2055.
(32) Fery-Forgues, S.; Le Bris, M.-T.; Guetté, J.-P.; Valeur, B. *J. Phys. Chem.* **1988**, *92*, 6233.
(33) Rurack, K.; Rettig, W.; Resch-Genger, U. *Chem. Commun.* **2000**, 407.
(34) Schmittel, M.; Ammon, H. *J. Chem. Soc., Chem. Commun.* **1995**, 687.
(35) Das, S.; Thomas, K. G.; Thomas, K. J.; Kamat, P. V.; George, M. V. *J. Phys. Chem.* **1994**, *98*, 9291.
(36) Akkaya, E. U. In *Chemosensors for Ion and Molecule Recognition*; Desvergne, J. P., Czarnik, A. W., Eds.; Nato ASI Series, Vol. 492; Kluwer Academic Publishers: Dordrecht, Netherlands, 1997; p 177.
(37) Oguz, U.; Akkaya, E. U. *Tetrahedron Lett.* **1997**, *38*, 4509.
(38) Marcotte, N.; Fery-Forgues, S.; Lavabre, D.; Marguet, S.; Pivovarenko, V. G. *J. Phys. Chem. A* **1999**, *103*, 3163.
(39) Marcotte, N.; Lavabre, D.; Fery-Forgues, S. *New J. Chem.*, submitted for publication, 2003.
(40) Doroshenko, A. O.; Grigorovich, A. V.; Posokhov, E. A.; Pivovarenko, V. G.; Demchenko, A. P. *Mol. Eng.* **1999**, *8*, 199.
(41) Doroshenko, A. O.; Grigorovich, A. V.; Posokhov, E. A.; Pivovarenko, V. G.; Demchenko, A. P.; Sheiko, A. D. *Russ. Chem. Bull.* **2001**, *50*, 404.
(42) Marcotte, N.; Fery-Forgues, S. *J. Photochem. Photobiol., A: Chem.* **2000**, *130*, 133.
(43) Dix, J. P.; Vögtle, F. *Chem. Ber.* **1980**, *113*, 457.
(44) Olomucki, M.; Le Gall, J. Y. *Bull. Soc. Chim. Fr.* **1976**, 1467.
(45) Reynolds, G. A.; Drexhage, K. H. *Opt. Commun.* **1975**, *13*, 222.
(46) Dai Hung, N.; Plaza, P.; Martin, M. M.; Meyer, Y. H. *Appl. Opt.* **1992**, *31*, 7046.
(47) Barnabas, M. V.; Liu, A.; Trifunac, A. D.; Krongauz, V. V.; Chang, C. T. *J. Phys. Chem.* **1992**, *96*, 212.
(48) Kahlaf, A. A.; Etaiw, S. H.; Issa, R. M.; El-Shafei, A. K. *Rev. Roum. Chim.* **1977**, *22*, 1251.
(49) Marcotte, N.; Fery-Forgues, S. *J. Chem. Soc., Perkin Trans. 2* **2000**, 1711.
(50) Harvey, P. D.; Gan, L.; Aubry, C. *Can. J. Chem.* **1990**, *68*, 2278.
(51) Harvey, P. D.; Aubry, C.; Gan, L.; Drouin, M. *J. Photochem. Photobiol., A: Chem.* **1991**, *57*, 465.
(52) Fery-Forgues, S.; Delavaux-Nicot, B.; Lavabre, D.; Rurack, K. *J. Photochem. Photobiol., A: Chem.*, in press.
(53) Horng, M. L.; Gardecki, J. A.; Papazyan, A.; Maroncelli, M. *J. Phys. Chem.* **1995**, *99*, 17311.
(54) Martin, M. M.; Plaza, P.; Meyer, Y. H. *Chem. Phys.* **1995**, *192*, 367.
(55) DeVoe, R. J.; Sahyun, M. R. V.; Schmidt, E.; Sadrai, M.; Serpone, N.; Sharma, D. K. *Can. J. Chem.* **1989**, *67*, 1565.
(56) Das, P. K.; Pramanik, R.; Banerjee, D.; Bagchi, S. *Spectrochim. Acta, Part A* **2000**, *56*, 2763.
(57) Pivovarenko, V. G.; Kleva, A. V.; Doroshenko, A. O.; Demchenko, A. P. *Chem. Phys. Lett.* **2000**, *325*, 389.
(58) Yamashita, K.; Imahashi, S. *J. Photochem. Photobiol., A: Chem.* **2000**, *135*, 135.
(59) Wang, Y. *J. Phys. Chem.* **1985**, *89*, 3799.
(60) Kaps, K.; Rentrop, P. *Comput. Chem. Eng.* **1984**, *8*, 393.
(61) Minoux, M. *Programmation Mathématique*; *Tome 1*; Dunod: Paris, 1983.